Macromolecules

Article

pubs.acs.org/Macromolecules

Effect of Oligothiophene π-Bridge Length on the Photovoltaic Properties of D−A Copolymers Based on Carbazole and Quinoxalinoporphyrin

Shaowei Shi,[†] Pei Jiang,[†,‡] Song Chen,[§] Yeping Sun,[†] Xiaochen Wang,[†] Kai Wang,[†] Suling Shen,[‡] Xiaoyu Li,*[,†] Yongfang Li,*[,‡] and Haiqiao Wang*[,†]

[†]State Key Laboratory of Organic−Inorganic Composite, Key Laboratory of Carbon Fiber and Functional Polymers, Ministry of Education, Beijing University of Chemical Technology, Beijing 100029, China

[‡]CAS Key Laboratory of Organic Solids, Institute of Chemistry, Chinese Academy of Sciences, Beijing 100190, China

[§]China Textile Academy, Beijing 100025, China

Supporting Information

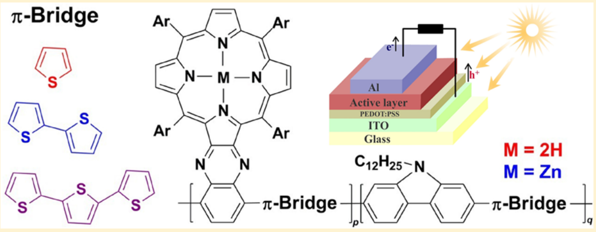

ABSTRACT: A series of low-bandgap donor−acceptor (D−A) copolymers, P(C-T-QP), P(C-BT-QP), P(C-TT-QP), and P(C-TT-QP-Zn), using 2,7-carbazole (C) as an electron-rich unit and quinoxalino[2,3-*b*′]porphyrins (QP) or quinoxalino[2,3-*b*′]-porphyrinatozinc(QP-Zn) as an electron-deficient unit with different length of oligothiophene π-bridges, were designed and synthesized via a Pd-catalyzed Stille-coupling method. The π-bridge between the C donor unit and the QP acceptor unit is thiophene (T) in P(C-T-QP), bithiophene (BT) in P(C-BT-QP), and terthiophene (TT) in P(C-TT-QP) or P(C-TT-QP-Zn). These copolymers possess good solubility, high thermal stability, broad absorption, and low bandgap ranging from 1.66 to 1.73 eV. The influence of the π-bridge and the central Zn ion on the electronic and photovoltaic properties was investigated and discussed in detail. It was found that the π-bridge played an important role in tuning the effective conjugation length and therefore significantly affected the molecular architecture and optoelectronic properties of the copolymers. With the π-bridge varying from thiophene to bithiophene, then to terthiophene, the hole mobility of the copolymers increased gradually, and the absorption was broadened in turn. Zn ion in the porphyrin ring also had a significant influence on the physicochemical and photovoltaic properties. Bulk heterojunction solar cells with the polymers as donor and $PC_{71}BM$ as acceptor demonstrated PCEs of 0.97% for P(C-T-QP), 1.97% for P(C-BT-QP), 2.53% for P(C-TT-QP), and 1.45% for P(C-TT-QP-Zn). All of them are among the highest PCE values of PSCs based on porphyrin polymers. Among the four polymers, although the P(C-TT-QP-Zn) shows the highest hole mobility and the widest absorption, the corresponding PSC demonstrated the lowest PCE because the morphology of P(C-TT-QP-Zn)/$PC_{71}BM$ blend film is not beneficial to the exciton dissociation and charge carriers transport. This study provides a new insight toward the design and future development of quinoxalinoporphyrin-based conjugated polymers.

■ INTRODUCTION

Bulk heterojunction (BHJ) polymer solar cells (PSCs) which are based on solution-processable conjugated polymer donor and fullerene derivative acceptor materials have been widely studied due to their low-cost solution fabrication process, lightweight, and device mechanical flexibility as well as potential contribution to clean and renewable energy. To achieve high-performance PSCs, the electron-donating conjugated polymers need to have appropriate band gaps to maximize solar radiation capture, good hole mobility, and reasonable highest occupied molecular orbital levels (HOMO) to maximize the short circuit current (J_{sc}) and open-circuit voltage (V_{oc}), respectively.[1−11] At present, conjugated polymers with electron donor−acceptor (D−A) architecture are particularly attractive due to the facile tunability of their electronic structure of the main chain by controlling the intramolecular charge transfer (ICT) from the donor units to the acceptor units.[12,13]

Porphyrins and their derivatives have been intensively studied over many years due to their importance in the photochemistry and biochemical processes. Porphyrins are preferable photosensitizers for utilizing solar energy for the reason that they play an important role in the photosynthesis of plants. Their large π-conjugation systems as well as their good thermal stabilities also make porphyrins to be promising materials for organic photonic and electronic applications.[14] Up to now, porphyrin-based small molecules BHJ solar cells and dye-sensitized solar cells (DSSCs) have reached power conversion efficiencies (PCEs) of more than 5% and 12%, respectively.[15,16] However, when applying porphyrin polymers in solar cells, poor PCEs were obtained (less than 1%).[17−23]

Received: July 11, 2012
Revised: September 10, 2012
Published: September 19, 2012

Scheme 1. Synthetic Route of the Monomers and Copolymers

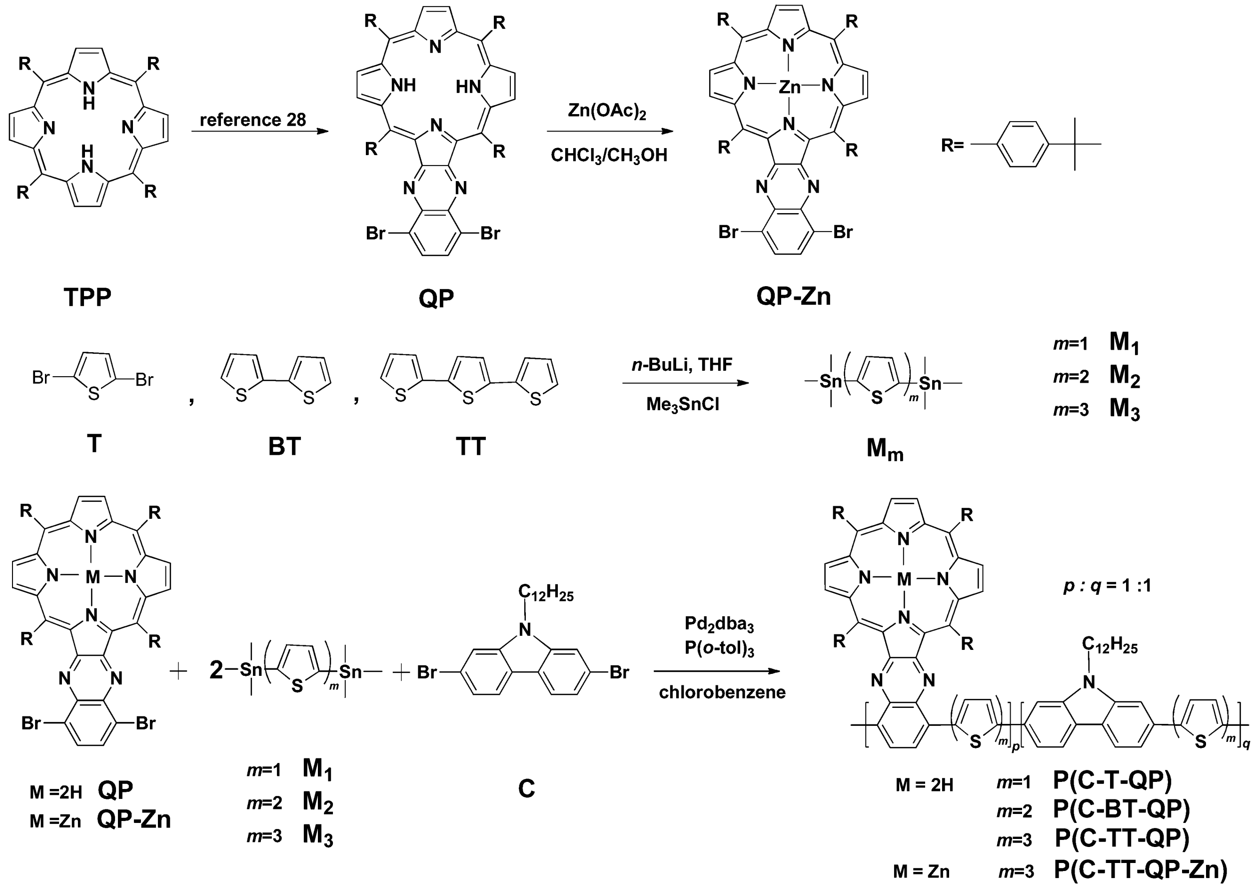

The relatively narrow absorption spectrum and less efficient conjugation in the main chain are the critical factors that limit the improvement of photoelectric properties. The typical absorption spectra of porphyrin units exhibit a sharp and strong Soret band (410−430 nm) and weak Q-bands (530−540 nm) without absorption between them, and the conventional meso-aryl linkage in porphyrin polymers cannot broaden the absorption effectively by intramolecular charge transfer (ICT) due to the large aryl−porphyrin dihedral angles.[23−25] However, quinoxalino[2,3-*b*′]porphyrins are more π-expanded systems and were proposed as "molecular wires".[26] By incorporation of different central metal ions or selective functionalization at β-pyrrolic positions, it enable "fine-tuning" of electronic properties of compounds by altering relative energy levels of the HOMO and lowest unoccupied molecular orbital (LUMO). But, the studies about quinoxalinoporphyrin are still at the level of small molecules or large multiporphyrin arrays, and it has not yet been used in polymers.[27] Recently, we designed and reported a new D-π-A copolymer P(C-TT-QP) with quinoxalinoporphyrin as acceptor unit, 2,7-carbazole as donor unit, and terthiophene as a π-bridge. P(C-TT-QP) exhibited an unusually broadened and enhanced Q-band absorbance compared to other porphyrin-based conjugated polymers reported in the literature. More interestingly, the absorption blank between the Soret band and Q-bands has been covered perfectly for the first time. As a result, PCE of solar cell based on P(C-TT-QP) reached 2.5%.[28] These results indicate that the photovoltaic performance of the porphyrin-based conjugated polymers could be greatly improved by using quinoxalinoporphyrin. However, to achieve higher efficiency porphyrin polymers, it is needed to further study the effect of the molecular structure on the optical, electrochemical, and photovoltaic properties.[29]

Herein, two novel quinoxalinoporphyrin-based copolymers P(C-T-QP) and P(C-BT-QP) were synthesized. Combining with our previously reported P(C-TT-QP), the three copolymers were used to systematically study the effects of the bridges on absorption, energy levels, and charge transport properties of the copolymers.

On the other hand, it is noted that nearly in all the literatures reported for the porphyrin-based photovoltaic polymers so far, zinc(II) porphyrins rather than free-base porphyrins were chosen as building blocks without discussion on their difference in photovoltaic properties. But Wong et al. reported that by blending free-base porphyrin additives in the 9,9-dioctylfluorenyl hexa-peri-hexabenzocoronene (FHBC) moiety, the performance of BHJ devices functioned better than the zinc(II) porphyrin additives.[30] Thus, it is of prime importance to fully understand the effect of the central Zn ion on the physicochemical and photovoltaic properties in the design of new porphyrin polymers for efficient PSCs. Herein, P(C-TT-QP-Zn) with Zn ion in the porphyrin ring of P(C-TT-QP) was also synthesized to comparably study the effects of the central metal ion with P(C-TT-QP). We found that conjugated bridges and central Zn ion in porphyrin ring crucially influence the electronic structure of polymer main chain and the interaction between donor and acceptor units and therefore remarkably affect coplanarity and optical, electrochemical, charge transport, and photovoltaic properties of the D-π-A conjugated copolymers.

RESULTS AND DISCUSSION

Synthesis and Thermal Stability. The synthesis routes of monomers and corresponding polymers are outlined in Scheme 1. Monomer QP was reacted with zinc acetate to give compound QP-Zn in a good yield. All polymers were synthesized by palladium-catalyzed Stille-coupling polymerization and purified by sequential Soxhlet extraction with methanol, hexanes, and $CHCl_3$. The $CHCl_3$ fraction was then reduced in volume, precipitated into methanol, and collected by filtration, yielding black or dark blue solids. P(C-T-QP), P(C-BT-QP), and P(C-TT-QP) can be readily dissolved in common solvents, such as chloroform, toluene, tetrahydrofuran (THF), and chlorobenzene, and processed to form smooth and pinhole-free films upon spin-coating. P(C-TT-QP-Zn) shows slight poor solubility but also can be dissolved in hot solvents. The molecular weight of the polymer was determined by GPC in THF solution relative to polystyrene standards, and the detailed GPC data are listed in Table 1. The thermal properties of the polymers were determined by thermogravimetric analysis (TGA) under a nitrogen atmosphere at a heating rate of 10 °C/min, as shown in Figure 1. All polymers have good thermal stability with onset decomposition temperatures with 5% weight loss at 426–456 °C and P(C-TT-QP-Zn) processes the highest. Obviously, the thermal stability of these polymers is adequate for their applications in PSCs and other optoelectronic devices.

Table 1. Molecular Weights and Thermal Properties of the Copolymers

polymer	M_n[a]	M_w[b]	PDI (M_w/M_n)[a]	T_d (°C)[b]
P(C-T-QP)	3.4K	5.2K	1.52	423
P(C-BT-QP)	51.5K	73.2K	1.42	435
P(C-TT-QP)	61.1K	130.3K	2.13	440
P(C-TT-QP-Zn)	66.4K	138.1K	2.08	456

[a] M_n, M_w, and PDI of the polymers were determined by gel permeation chromatography using polystyrene standards in THF. [b] The 5% weight-loss temperatures in the air.

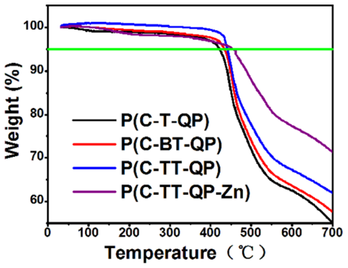

Figure 1. TGA plots of the polymers with a heating rate of 10 °C/min under an inert atmosphere.

Optical Properties. The absorption spectra of all studied polymers were measured in both dilute chloroform and the thin films (Figure 2a–d), and the correlated optical parameters are summarized in Table 2, including the absorption peak wavelengths (λ_{abs}), the absorption edge wavelengths (λ_{onset}), and the optical band gap (E_g^{opt}). For the convenience of study, we also measured the absorption spectrum of monomers TPP, QP, and QP-Zn as references. It is noted that when edge-fusing porphyrin with quinoxaline, the Soret bands of QP and QP-Zn are significantly broadened due to the extension π-conjugation (see Figure 2a,c). All the polymers show absorptions in the regions of Soret band and Q-bands. Compared to the reference QP and QP-Zn absorption, the Soret band and Q-bands of the polymers are both broadened while the Q-bands enhance observably. The blank between the Soret and Q-bands is filled completely. And the absorption areas between the Soret and Q-bands increase gradually with the oligothiophene bridges varying from thiophene to bithiophene and then to terthiophene due to more extended π-conjugation resulting in a more effective ICT effect. The results demonstrate that the effective ICT effect along the main chain of polymers is the key factor to broaden and enhance Q-band absorbance and fill blank absorption. The absorption spectra of the four polymers in the solid state are all broadened compared to their corresponding solution spectra. However, only slight red-shifts (ca. 1–5 nm) of their absorption maxima are obtained, which is probably due to the bulky 4-*tert*-butylphenyl substituents on the porphyrins that prevent aggregation in the solid state.[30] In Figure 2a,b, it is clear that the absorption spectra of P(C-T-QP), P(C-BT-QP), and P(C-TT-QP) vary with the number of the conjugated thiophene rings. A comparison of the polymers reveals that P(C-TT-QP) exhibits the most bathochromic shift of the absorption maximum at 438 nm in the chloroform solution, whereas P(C-T-QP) exhibited the most hypsochromic shift absorption maximum at 427 nm. The absorption edges for solid films of P(C-T-QP), P(C-BT-QP), and P(C-TT-QP) increase from 679, 736, to 742 nm, corresponding to optical band gaps (E_g^{opt}) decreasing from 1.83, 1.68, to 1.67 eV, respectively. The decreasing in E_g^{opt} from P(C-T-QP) to P(C-BT-QP) and to P(C-TT-QP) can attribute to the presence of a more extended and delocalized π-electron system (in both solutions and solid films) which extends the conjugation lengths of the copolymers and reduces the band gap. Also, increasing in the length of the oligothiophene bridges is beneficial to decrease steric hindrance between QP and its neighboring units.

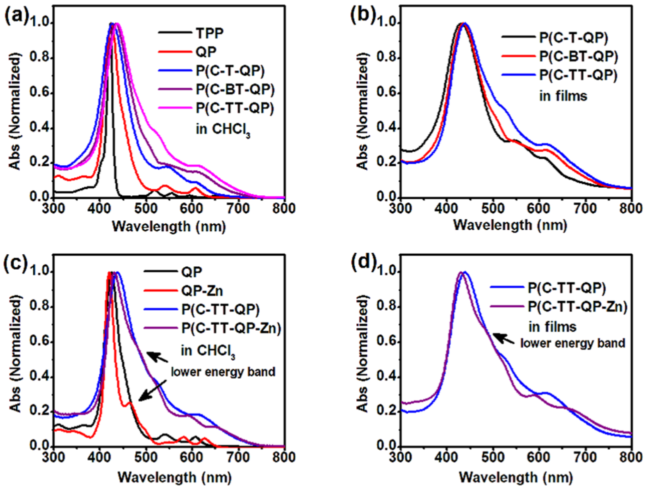

Figure 2. UV–vis spectra of copolymers and reference monomers in $CHCl_3$ solutions and in thin films.

In Figure 2c,d, although the absorption maxima of P(C-TT-QP) and QP slightly red-shift more than P(C-TT-QP-Zn) and QP-Zn both in solution and in solid film, P(C-TT-QP-Zn) and QP-Zn possess more bathochromic Q-bands, and the absorption edges of P(C-TT-QP-Zn) red-shift ca. 7 nm compared to P(C-TT-QP). It can be noticed that there are individually identifiable two components of the Soret band in

Table 2. Optical and Electrochemical Properties of the Polymers

polymer	λ_{abs} in solution[a] (nm)	λ_{abs} in film[b] (nm)	λ_{emi} in solution[a] (nm)	λ_{onset} in film (nm)	$E_g^{opt\ c}$ (eV)	HOMO/E_{ox}(eV)/(V)	LUMO (eV)
P(C-T-QP)	427	431	708	717	1.73	−5.39/0.68	−3.66
P(C-BT-QP)	435	434	734	736	1.69	−5.36/0.65	−3.68
P(C-TT-QP)	438	439	744	742	1.67	−5.33/0.62	−3.66
P(C-TT-QP-Zn)	431	430	755	749	1.66	−5.24/0.53	−3.58

[a] Measured in chloroform solution. [b] Cast from chlorobenzene solution. [c] Bandgap estimated from the onset wavelength (λ_{onset}) of the optical absorption: E_g^{opt} = 1240 nm·eV/λ_{onset}.

QP-Zn with one of these moving to lower energy compared to the free-base analogue, and it is clear that the lower-energy Soret component shows low intensity. This feature is retained in the spectrum of P(C-TT-QP-Zn) with a shoulder at ca. 500 nm. The reason for this phenomenon is somewhat complicated, and further study is ongoing. But at least we can infer that QP-Zn shows more extended π-conjugation than the free-base analogue.

The normalized photoluminescence (PL) spectra of the polymers in $CHCl_3$ solution (at concentration of 1 mg/100 mL) are shown in Figure 3. The solution PL spectra of all polymers reveal both emission from donor segment (450−600 nm) and from the porphyrin moiety (650−800 nm), which is indicative of incomplete energy transfer from the polymer backbone to QP or QP-Zn unit. Also, it is clear that the PL intensity of P(C-TT-QP-Zn) is lower than those of other three polymers which means weaker energy transfer when incorporate Zn ion in QP. The emission peak wavelengths λ_{emi} of P(C-T-QP), P(C-BT-QP), and P(C-TT-QP) are consistent with the trend of λ_{abs} in their corresponding absorption spectra. P(C-TT-QP-Zn) shows the largest bathochromic-shifted spectrum with maximum emission at 755 nm compared to P(C-TT-QP), which is corresponding to the red-shifted Soret band.

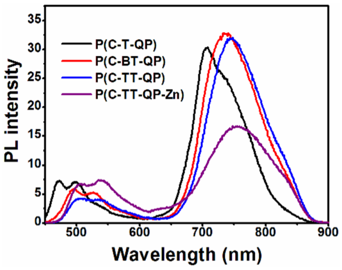

Figure 3. Photoluminescence spectra of the polymers in chloroform solution (excited at 430 nm) at concentration of 1 mg/100 mL.

Electrochemical Properties. Cyclic voltammetry (CV) has been employed and considered as an effective tool in investigating electrochemical properties of conjugated oligomers and polymers.[31] Cyclic voltammograms of the polymer films are shown in Figure 4. The energy levels of the HOMO and LUMO of the polymers were calculated according to the equations[32]

$$\mathrm{HOMO} = -\mathrm{IP} = -e(E_{ox} + 4.71)\ (\mathrm{eV}) \qquad (1)$$

$$\mathrm{LUMO} = E_g^{opt} + \mathrm{HOMO}\ (\mathrm{eV}) \qquad (2)$$

From the value of onset oxidation potential (E_{ox}) and E_g^{opt} of the polymers, the HOMO and the LUMO were calculated and are listed in Table 2. The moderate onset oxidation potentials of P(C-T-QP), P(C-BT-QP), and P(C-TT-QP) are determined to be 0.68, 0.65, and 0.62 V vs Ag/Ag$^+$, respectively, corresponding with the HOMO levels to be −5.39, −5.36, and −5.33 eV. It was worthwhile to note that the HOMO energy levels of the three polymers increase with the increasing conjugation length. The copolymers possess comparable LUMO levels between −3.66 and −3.68 eV, demonstrating that the LUMO levels of the QP-based polymers are mainly dominated by the QP unit.[31b] Compared to P(C-TT-QP), P(C-TT-QP-Zn) shows higher HOMO/LUMO energy levels, which can be attributed to the increased electron density, and it can be inferred that the electron-accepting ability of QP-Zn is weaker than QP.[30] Since the open circuit voltage V_{oc} of BHJ PSCs is correlated to the difference between the LUMO energy level of the fullerene and HOMO energy level of the donor polymer, therefore a reasonable V_{oc} for QP or QP-Zn-based PSCs is anticipated due to the low-lying HOMO energy level. On the other hand, the LUMO energy levels of these polymers are located at reasonable positions from −3.66 to −3.68 eV which offer enough driving force for charge separation and transfer without too much energy loss.[13]

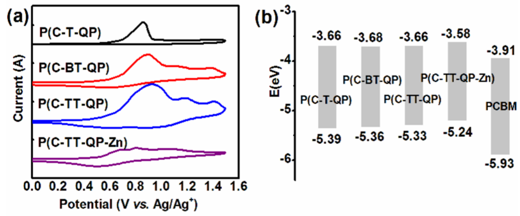

Figure 4. (a) Cyclic voltammograms of the polymer films on Pt electrode in 0.1 mol/L Bu_4NPF_6, CH_3CN solution with a scan rate of 100 mV/s. (b) Energy level diagrams for P(C-T-QP), P(C-BT-QP), P(C-TT-QP), and P(C-TT-QP-Zn).

Theoretical Calculations. To provide further insight into the fundamentals of molecular architecture, molecular simulation was carried out for P(C-TT-QP) and P(C-TT-QP-Zn). The molecular geometries of the two polymers were optimized in a trans conformation, with a chain length of $n = 1$ at the B3LYP/6-31G(d,p) level with the GAMESS program package.[33] The alkyl chain of carbazole was replaced by methyl group, and 4-*tert*-butylphenyl at 10 and 15 positions of QP or QP-Zn was replaced by phenyl group in the calculation to avoid excessive computation demand. To better study the effects of substituents on the structure of the main chain, 4-*tert*-butylphenyl at 5 and 20 positions was retained (as shown in Figure 5).

The wave functions of the frontier molecular orbital are depicted in Figure 6. As can be observed, the HOMO is delocalized along the whole π-conjugated backbone while the LUMO is mostly concentrated on the quinoxalinoporphyrin-based acceptor groups. These images provide further evidence of the formation of well-defined D-π-A structure and the ICT

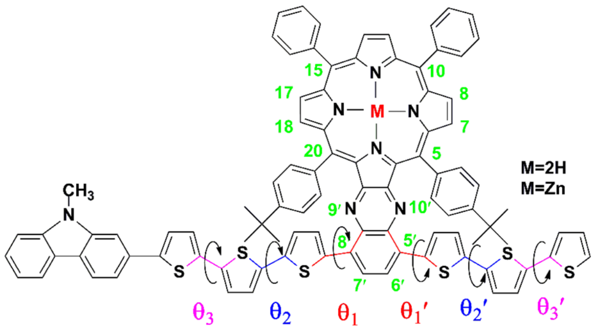

Figure 5. Molecular geometry sketch used for the computational data.

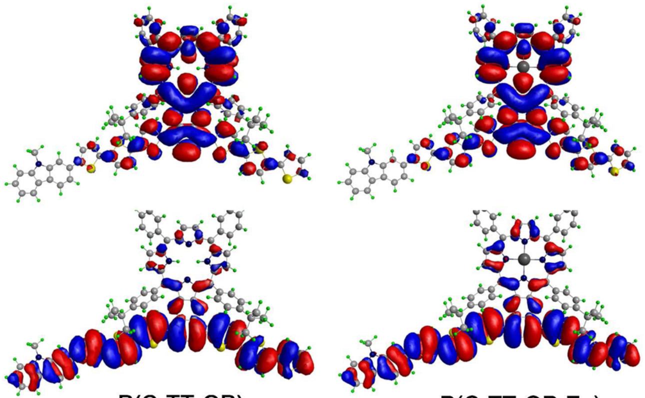
P(C-TT-QP) P(C-TT-QP-Zn)

Figure 6. Frontier molecular orbital (LUMO, top; HOMO, bottom) obtained from density functional theory (DFT) calculations on the polymers with a chain length *n* = 1 at B3LYP/6-31G(d,p) level of theory.

behavior of the material (i.e., the HOMO to LUMO transition is a donor to acceptor intramolecular charge transfer).[34] The optimized geometries are shown in Figure 7, and relevant dihedral angles are listed in Table 3. All the dihedral angles are relatively small which is benefical to form a better planar conjugated polymer backbone. Also, we can notice that terthiophene and bithiophene are more helpful to decrease the steric hindrance from the 4-*tert*-butylphenyls of meso positions, and this can partly explain the lower molecule weight of P(C-T-QP) relative to that of P(C-BT-QP) and P(C-TT-QP). The difference of the dihedral angles between P(C-TT-QP) and P(C-TT-QP-Zn) is slight, which demonstrates the complexing of zinc has not a remarkable influence on the architecture of the polymers.

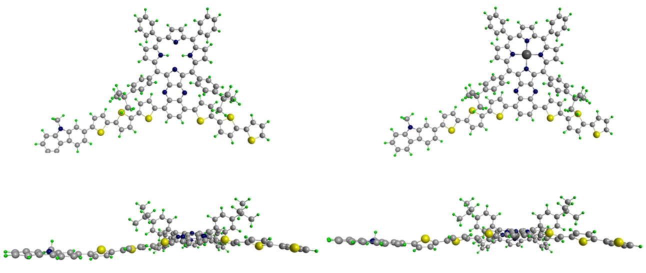
P(C-TT-QP) P(C-TT-QP-Zn)

Figure 7. Top view (top) and side view (bottom) of optimized structures of the copolymers backbone units with a chain length *n* = 1.

Table 3. Calculated Dihedral Angles of Polymers

polymer	θ_1	θ_2	θ_3	θ_1'	θ_2'	θ_3'
P(C-TT-QP)	−20.03	7.73	−14.84	18.84	6.98	−16.41
P(C-TT-QP-Zn)	−19.07	6.67	−13.41	18.09	6.08	−17.03

Photovoltaic Properties. To investigate the effects of π-conjugated bridges and zinc on the photovoltaic properties of the copolymers, BHJ PSC devices with a configuration of ITO/PEDOT:PSS/polymer:$PC_{71}BM$/Ca/Al were fabricated. Figure 8 shows the current density−potential characteristic of PSCs based on the blends of polymer:$PC_{71}BM$ under illumination of AM1.5G, 100 mW/cm^2. To further study the performance of the PSCs devices, the hole mobilities in the photosensitive layers were measured by the space charge limited current (SCLC) method using devices with structure of ITO/PEDOT:PSS/polymer:$PC_{71}BM$/Au. For unipolar transport in a trap-free semiconductor with an ohmic injecting contact, the SCLC can be approximated by the Mott−Gurney equation:

$$J \cong \frac{9}{8}\varepsilon_r\varepsilon_0\mu_0 \exp\left(0.891\gamma\sqrt{\frac{V}{L}}\right)\frac{V^2}{L^3} \qquad (3)$$

where J is the current density, ε_r is the dielectric constant of the polymer, ε_0 is the free-space permittivity (8.85×10^{-12} F/m), μ_0 is the charge mobility at zero field, γ is a constant, L is the thickness of the blended film layer, $V = V_{appl} - V_{bi}$, V_{appl} is the applied potential, and V_{bi} is the built-in potential which results from the difference in the work function of the anode and the cathode (in this device structure, V_{bi} = 0.2 V). Figure 9 displays $\ln(JL^3/V^2)$ versus $(V/L)^{0.5}$ curve for the measurement of the hole mobility of the copolymers by the SCLC method. As summarized in Table 4, the hole mobilities of the polymers calculated using eq 3 are 3.1×10^{-6}, 9.6×10^{-6}, 3.3×10^{-5}, and 1.3×10^{-4} cm^2 V^{-1} s^{-1} for P(C-T-QP), P(C-BT-QP), P(C-TT-

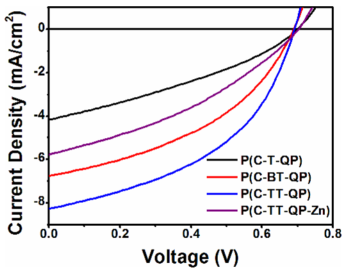

Figure 8. Current density−potential characteristic of PSCs based on polymer:$PC_{71}BM$ under illumination of AM1.5G, 100 mW/cm^2.

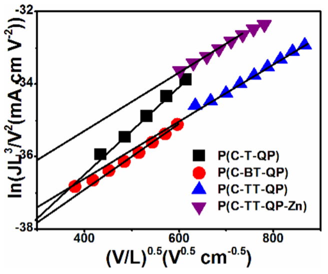

Figure 9. Plots of $\ln(JL^3/V^2)$ versus $(V/L)^{0.5}$ for the measurement of the hole mobility in polymer/$PC_{71}BM$ devices by the SCLC method.

Table 4. Photovoltaic Performances of the PSCs Based on Polymer/$PC_{71}BM$ under the Illumination of AM1.5, 100 mW/cm^2

polymer	polymer/$PC_{71}BM$ (w/w)	V_{oc} (V)	J_{sc} (mA/cm^2)	FF	PCE (%)	mobility (cm^2 V^{-1} s^{-1})
P(C-T-QP)	1:2	0.69	4.15	0.34	0.97	3.1×10^{-6}
P(C-BT-QP)	1:3	0.68	6.80	0.43	1.97	9.6×10^{-6}
P(C-TT-QP)	1:3	0.68	8.32	0.45	2.53	3.3×10^{-5}
P(C-TT-QP-Zn)	1:3	0.70	5.79	0.36	1.45	1.3×10^{-4}

QP), and P(C-TT-QP-Zn), respectively. It can be noticed that P(C-T-QP) and P(C-BT-QP) show lower hole mobilities than P(C-TT-QP). This variation in device behavior can be attributed to the change of the coplanarity in the polymer backbone by the introduction of various oligothiophene bridges, and we can conclude that the change of the π-bridge from thiophene to bithiophene, and then to terthiophene, results in gradully increase of the intrachain mobility because of more extended π-conjugation and less steric hindrance. P(C-TT-QP-Zn) shows the highest hole mobility of the order of 10^{-4} cm^2 V^{-1} s^{-1}, indicating that the incorporation of zinc may be in favor of enhancing the packing structure in the blends.

The V_{oc}, J_{sc}, fill factor (FF), PCE, and hole mobility of the PSCs are summarized in Table 4. An obvious increase in the J_{sc} and PCE can be observed from P(C-T-QP) to P(C-TT-QP) (i.e., P(C-T-QP) < P(C-BT-QP) < P(C-TT-QP)). The J_{sc} of the polymers increased from 4.15, 6.80, to 8.32 mA/cm^2, which is consistent with the lowered band gaps (from 1.73, 1.68, to 1.67 eV). The optimum photovoltaic performance with the maximum PCE value of 2.53% (V_{oc} = 0.68 V, J_{sc}= 8.32 mA/cm^2, FF = 0.45) was obtained in the PSC device having a weight ratio of P(C-TT-QP):$PC_{71}BM$ = 1:3. When complexing zinc in the center, P(C-TT-QP-Zn) shows lower FF(0.36) and J_{sc} (5.79) compared to P(C-TT-QP) and a PCE of 1.45% is obtained. Figure 10 shows the external quantum efficiencies (EQE) curves of the devices incorporating the polymer:$PC_{71}BM$ blends. It is apparent that all devices exhibited a broad response range, covering from 300 to 750 nm with maximum EQE values of 37% at ~465 nm, 48% at ~475 nm, and 51% at ~460 nm for the PSCs based on P(C-T-QP), P(C-BT-QP), and P(C-TT-QP), respectively. Compared to the absorption spectra of pristine polymers, the significantly broadened EQE responses in the visible region can be attributed to both the intrinsic absorptions of the polymers and $PC_{71}BM$. P(C-TT-QP)-based device improved the EQE upon that of P(C-T-QP) and P(C-BT-QP) markedly, especially in the range of 400−500 nm. It is remarkable to see that the light-harvesting ability of P(C-TT-QP) (with its commensurately high charge mobilities and favorable light absorption characterisitics) can be increased by introducing terthiophene in the main chain. This is in agreement with increased maximum absorption with increasing m from M_1 to M_3, resulting in higher PCE for the polymers.[29a−e] P(C-TT-QP-Zn) showed lower EQE than P(C-TT-QP) with maximum EQE value of 44% at ~480 nm. Additionally, a less than 10% difference between the J_{sc} and the integral of the EQE is observed. Since the EQE was tested in the air, this discrepancy should be mainly ascribed to the degradation caused by the oxidation of the Ca electrode.

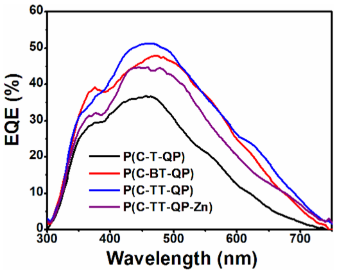

Figure 10. EQE spectra of the PSCs based on polymer:$PC_{71}BM$ blends.

We noted that Wong et al. also found the zinc porphyrin derivative functioned worse in solar cells than the free-base porphyrin derivatives,[30] and they attributed the poor performance of solar cell to the less stable of zinc porphyrin. However, in this work, we observed that the zinc porphyrin polymer possesses better thermal stability than their free-base analogues. Considering the fact that the P(C-TT-QP-Zn) possesses the highest hole mobility and the strongest and the widest absorption among the four polymers, herein, we conjectured the possible reason for the worst performance of P(C-TT-QP-Zn)-based PSC is the film morphology of the P(C-TT-QP-Zn)/$PC_{71}BM$ blend.

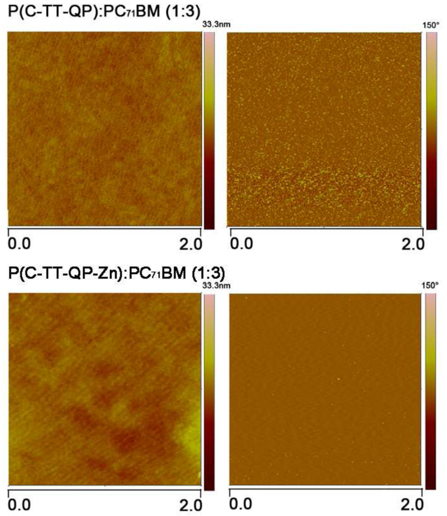

Figure 11. AFM topography (left) and phase (right) images of the blend films of polymer/$PC_{71}BM$; the size of the image is 2 μm × 2 μm.

In order to understand the effect of mophology of the photoactive layers on the photovoltaic performance of the polymer solar cells, the mophological structures of the blend films of polymer/$PC_{71}BM$ were analyzed by tapping mode atom force microscopy (AFM) measurements. Figure 11 shows the AFM images of the blend films. The blend films based on P(C-TT-QP) and P(C-TT-QP-Zn) both demonstrated low roughness of 1.05 and 1.29 nm, respectively. The P(C-TT-QP)/$PC_{71}BM$ blend possesses higher FF due to its smoother surface. For the P(C-TT-QP)/$PC_{71}BM$ blend film, the bright patterns of polymer domains showed a good interpenetrating network which is beneficial to the exciton dissociation and charge carriers transport. Obviously, the suitable morphology of the blend films are consistent with the higher photovoltaic performance of the PSCs based on P(C-TT-QP).

■ CONCLUSION

In conclusion, a series of quinoxalinoporphyrin-based D−A copolymers with carbazole as donor unit and oligothiophene as π-bridge have been synthesized and well characterized. These copolymers possess good solubility and high thermal stability as well as lower bandgap. We demonstrated that their electronic and photovoltaic properties can be easily tuned via the variation of oligothienyl chain π-bridge length, and we carefully studied the difference between zinc(II) porphyrin and free-base porphyrin for the first time. By changing the type of π-bridge, the absorption edges of P(C-T-QP), P(C-BT-QP), and P(C-TT-QP) in films red-shift from 717, 736, to 742 nm, and the band gaps of the polymers are tuned from 1.73, 1.68, to 1.67 eV by upshifting the HOMO from −5.39, −5.36, to −5.33 eV. When incorporating zinc in center of porphyrin, the HOMO/LUMO energy levels are upshifted and 1.66 eV of the band gap is obtained. The hole mobilities of P(C-T-QP), P(C-BT-QP), and P(C-TT-QP) increase from 3.1×10^{-6}, 9.6×10^{-6}, to 3.3×10^{-5} cm^2 V^{-1} s^{-1} while P(C-TT-QP-Zn) shows the highest hole mobility of 1.3×10^{-4} cm^2 V^{-1} s^{-1}, indicating that the incorporation of zinc may be propitious to enhancing the packing structure in the blends. The PCEs of the PSCs incorporating the polymers and PC$_{71}$BM reach to 0.97% (P(C-T-QP)), 1.97% (P(C-BT-QP)), 2.53% (P(C-TT-QP)), and 1.45% (P(C-TT-QP-Zn)). The hole mobilities and PCEs increase with the number of thiophene rings, showing that terthiophene is more beneficial for decreasing the degree of curvature in the polymer backbone and increasing the effective conjugation length. Preliminary research show that the complexing of zinc may be a disadvantage to the improvement of PCEs due to decreasing both short-circuit current and fill factor although zinc(II) porphyrin possesses higher hole mobility and better thermal stability, which could provide a new insight into the design and future development of porphyrin-based conjugated polymers.

■ EXPERIMENTAL SECTION

Synthesis. *General.* 2,7-Dibromo-9-dodecyl-9*H*-carbazole (CZ), 2,5-bis(trimethylstannyl)thiophene (M$_1$), 2,2′-bithiophene-5,5′-bis(trimethylstannane) (M$_2$), 2,2′:5′,2″-terthiophene-5,5″-bis(trimethylstannane) (M$_3$), and 5,10,15,20-tetrakis(4-*tert*-butylphenyl)-5′,8′-dibromoquinoxalino[2,3-*b*′]porphyrin (QP) were synthesized as reported in the literature.[28,34] Other reagents and solvents were commercial grade and used as received without further purification.

5,10,15,20-Tetrakis(4-tert-butylphenyl)quinoxalino[2,3-b′]-5′,8′-dibromoporphyrinatozinc (QP-Zn). A mixture of QP (495 mg, 0.45 mmol), zinc(II) acetate dihydrate (296 mg, 1.35 mmol), chloroform (100 mL), and methanol (30 mL) was heated at reflux for 3 h. The reaction mixture was allowed to cool and the solvent removed. Column chromatography on silica gel (hexane/CH$_2$Cl$_2$ = 1:1) afforded QP-Zn as a dark blue solid (492 mg, 94%). ^{1}H NMR (CDCl$_3$, 600 MHz) δ (ppm): δ1.61−1.65 (m, 36H), 7.76 (d, 4H), 7.83 (d, 4H), 7.99 (s, 2H), 8.12 (m, 8H), 8.72−8.93 (m, 6H). MS (MALDI-TOF) m/z 1162.5 (M + H$^+$).

Synthesis of Copolymers. *P(C-T-QP).* To a 25 mL two-necked flask were added monomer CZ (49 mg, 0.10 mmol), QP (110 mg 0.10 mmol), M$_1$ (82 mg, 0.2 mmol), and chlorobenzene (6 mL). The mixture was purged with nitrogen for 15 min, and then Pd$_2$(dba)$_3$ (10 mg, 0.01 mmol) and P(o-tol)$_3$ (25 mg, 0.08 mmol) were added. After being purged for 15 min, the reaction mixture was heated at 140 °C for 72 h. After being cooled to room temperature, the reaction mixture was added dropwise to 200 mL of methanol and then collected by filtration and washed with methanol. Then the solid was subjected to Soxhlet extraction with methanol, hexane, and chloroform. Subsequently, the fraction that was extracted by chloroform was evaporated under reduced pressure and then precipitated in methanol, filtered, and finally dried under vacuum to obtain a black solid (60 mg, yield 41%, M_n = 3.4 kDa, M_w = 5.2 kDa, PDI = 1.52). ^{1}H NMR (CDCl$_3$, 600 MHz) δ (ppm): δ −2.34 to −2.24 (br, NH), 0.75−2.62 (br, alkyl-H), 3.75−4.52 (br, alkyl-H), 7.30−8.55 (br, Ar−H), 8.67−9.10 (br, pyrrolic-H). Elemental analysis: Calcd for C$_{98}$H$_{99}$N$_7$S$_2$: C, 81.80; H, 6.93; N, 6.81; S, 4.46. Found: C, 79.77; H, 6.836; N, 6.530; S, 4.245.

P(C-BT-QP). To a 25 mL two-necked flask were added monomer CZ (49 mg, 0.10 mmol), QP(110 mg 0.10 mmol), M$_2$ (98 mg, 0.2 mmol), and chlorobenzene (6 mL). The mixture was purged with nitrogen for 15 min, and then Pd$_2$(dba)$_3$ (10 mg, 0.01 mmol) and P(o-tol)$_3$ (25 mg, 0.08 mmol) were added. After being purged for 15 min, the reaction mixture was heated at 140 °C for 72 h. After being cooled to room temperature, the reaction mixture was added dropwise to 200 mL of methanol and then collected by filtration and washed with methanol. Then the solid was subjected to Soxhlet extraction with methanol, hexane, and chloroform. Subsequently, the fraction that was extracted by chloroform was evaporated under reduced pressure and then precipitated in methanol, filtered, and finally dried under vacuum to obtain a black solid (107 mg, yield 73%, M_n = 51.5 kDa, M_w = 73.2 kDa, PDI = 1.42). ^{1}H NMR (CDCl$_3$, 600 MHz) δ (ppm): δ −2.37 to −2.24 (br, NH), 0.53−2.35 (br, alkyl-H), 3.65−3.85 (br, alkyl-H), 7.10−8.45 (br, Ar−H), 8.70−9.23 (br, pyrrolic-H). According to the theoretical p/q ratio of 1:1. Elemental analysis: Calcd for C$_{106}$H$_{103}$N$_7$S$_4$: C, 79.41; H, 6.48; N, 6.12; S, 8.00. Found: C, 75.94; H, 6.414; N, 5.502; S, 7.747.

P(C-TT-QP-Zn). To a 25 mL two-necked flask were added monomer CZ (25 mg, 0.05 mmol), QP-Zn (58 mg 0.05 mmol), M$_3$ (57 mg, 0.1 mmol), and chlorobenzene (5 mL). The mixture was purged with nitrogen for 15 min, and then Pd$_2$(dba)$_3$ (5 mg, 0.005 mmol) and P(o-tol)$_3$ (13 mg, 0.04 mmol) were added. After being purged for 15 min, the reaction mixture was heated at 140 °C for 24 h. After being cooled to room temperature, the reaction mixture was added dropwise to 200 mL of methanol and then collected by filtration and washed with methanol. Then the solid was subjected to Soxhlet extraction with methanol, hexane, and chloroform. Subsequently, the fraction that was extracted by chloroform was evaporated under reduced pressure and then precipitated in methanol, filtered, and finally dried under vacuum to obtain a black solid (29 mg, yield 32%, M_n = 66.4 kDa, M_w = 138.1 kDa, PDI = 2.08). ^{1}H NMR (CDCl$_3$, 600 MHz) δ (ppm): 0.43−2.25 (br, alkyl-H), 3.60−3.79 (br, alkyl-H), 7.10−8.37 (br, Ar−H), 8.65−9.09 (br, pyrrolic-H). Elemental analysis: Calcd for C$_{114}$H$_{105}$N$_7$S$_6$Zn: C, 74.79; H, 5.78; N, 5.36; S, 10.51. Found: C, 71.50; H, 5.763; N, 4.922; S, 10.210.

Measurements and Characterization. The molecular weight of the polymer was measured using gel permeation chromatography (GPC). The GPC measurements were performed on Waters 515-2410 with polystyrenes as reference standard and THF as an eluent. All new compounds were characterized by nuclear magnetic resonance (NMR) spectra. The NMRs were recorded on a Bruker AV 600 spectrometer in CDCl$_3$ at room temperature. Chemical shifts of ^{1}H NMR were reported in ppm. Splitting patterns were designated as s (singlet), t (triplet), d (doublet), m (multiplet), and br (broaden). Matrix-assisted laser desorption/ionization time-of-flight (MALDI-TOF) mass spectra were made on a Shimadzu KOMPACT MALDI II using CHCA as a matrix. Elemental analyses were performed on a Flash EA 1112 analyzer or Elementar vario EL III. Thermal gravimetric analysis (TGA, NetzschTG209C) was performed under a nitrogen atmosphere at a heating rate of 10 °C/min. UV−vis absorption spectra were recorded on a Shimadzu spectrometer model UV-3150. Absorption spectra measurements of the polymer solutions were performed in chloroform (analytical reagent) at 25 °C. Absorption spectra measurements of the polymer films were performed on the quartz plates with the polymer films spin-coated from the polymer solutions in chlorobenzene (analytical reagent) at 25 °C. The electrochemical cyclic voltammetry was conducted on a Zahner IM6e electrochemical workstation with Pt disk coated with the polymer film, Pt plate, and Ag/Ag^+ electrode as working electrode, counter electrode, and reference electrode, respectively, in a 0.1 mol/L tetrabutylammonium hexafluorophosphate (Bu_4NPF_6)−acetonitrile solution.

Device Fabrication and Characterization of PSCs. PSCs were fabricated with ITO glass as a positive electrode, Ca/Al as a negative electrode, and the blend film of the polymer/$PC_{71}BM$ between them as a photosensitive layer. The ITO glass was precleaned and modified by a thin layer of PEDOT:PSS which was spin-cast from a PEDOT:PSS aqueous solution (Clevious P VP AI 4083 H.C. Stark, Germany) on the ITO substrate, and the thickness of the PEDOT:PSS layer is about 35 nm. The photosensitive layer was prepared by spin-coating a blend solution of polymers and PC71BM in *o*-dichlorobenzene on the ITO/PEDOT:PSS electrode. Then the Ca/Al cathode was deposited on the active layer by vacuum evaporation under 3×10^{-5} Pa. The effective area of one cell is 4 mm^2, and the thickness of the photosensitive layer is ca. 90 nm. The current−voltage ($J-V$) measurement of the devices was conducted on a computer-controlled Keithley 236 Source Measure Unit in drybox under inert atmosphere. A xenon lamp with AM 1.5 filter was used as the white light source, and the optical power at the sample was 100 mW/cm^2. The external quantum efficiency (EQE) was measured using a Stanford Research Systems model SR830 DSP lock-in amplifier coupled with a WDG3 monochromator and 500 W xenon lamp. The light intensity at each wavelength was calibrated with a standard single-crystal Si photovoltaic cell. All the measurements were performed under ambient atmosphere at room temperature.

■ ASSOCIATED CONTENT

Ⓢ Supporting Information

Figures S1 and S2. This material is available free of charge via the Internet at http://pubs.acs.org.

■ AUTHOR INFORMATION

Corresponding Author

*E-mail: wanghaiqiao@mail.buct.edu.cn (H.W.); liyf@iccas.ac.cn (Y.L.); lixy@mail.buct.edu.cn (X.L.).

Notes

The authors declare no competing financial interest.

■ ACKNOWLEDGMENTS

This work was financially supported by Beijing Natural Science Foundation (2122047).

■ REFERENCES

(1) (a) Thompson, B. C.; Fréchet, J. M. J. *Angew. Chem., Int. Ed.* **2008**, *47*, 58. (b) Beaujuge, P. M.; Fréchet, J. M. J. *J. Am. Chem. Soc.* **2011**, *133*, 20009.

(2) (a) Li, Y. *Acc. Chem. Res.* **2012**, *45*, 723. (b) Wong, W. Y.; Ho, C. L. *Acc. Chem. Res.* **2010**, *43*, 1246.

(3) Li, C.; Liu, M.; Pschirer, N. G.; Baumgarten, M.; Müllen, K. *Chem. Rev.* **2010**, *110*, 6817.

(4) (a) Cheng, Y.; Yang, S.; Hsu, C. *Chem. Rev.* **2009**, *109*, 5868. (b) Chen, J.; Cao, Y. *Acc. Chem. Res.* **2009**, *42*, 1709.

(5) Dennler, G.; Scharber, M. C.; Brabec, C. J. *Adv. Mater.* **2009**, *21*, 1323.

(6) Scharber, M. C.; Mühlbacher, D.; Koppe, M.; Denk, P.; Waldauf, C.; Heeger, A. J.; Brabec, C. J. *Adv. Mater.* **2006**, *18*, 789.

(7) Facchetti, A. *Chem. Mater.* **2011**, *23*, 733.

(8) (a) Zhou, H.; Yang, L.; You, W. *Macromolecules* **2012**, *45*, 607. (b) Chu, T.-Y.; Lu, J.; Beaupré, S.; Zhang, Y.; Pouliot, J.-R.; Wakim, S.; Zhou, J.; Leclerc, M.; Li, Z.; Ding, J.; Tao, Y. *J. Am. Chem. Soc.* **2011**, *133*, 4250.

(9) Brabec, C. J.; Gowrisanker, S.; Halls, J. J. M.; Laird, D.; Jia, S.; Williams, S. P. *Adv. Mater.* **2010**, *22*, 3839.

(10) (a) Chen, H.-Y.; Hou, J. H.; Zhang, S. Q.; Liang, Y. Y.; Yang, G. W.; Yang, Y.; Yu, L. P.; Wu, Y.; Li, G. *Nat. Photonics* **2009**, *3*, 649. (b) Liang, Y.; Yu, L. *Acc. Chem. Res.* **2010**, *43*, 1227. (c) Liang, Y.; Xu, Z.; Xia, J.; Tsai, S.-T.; Wu, Y.; Li, G.; Ray, C.; Yu, L. *Adv. Mater.* **2010**, *22*, E135.

(11) (a) Huo, L. J.; Zhang, S. Q.; Guo, X.; Xu, F.; Li, Y. F.; Hou, J. H. *Angew. Chem., Int. Ed.* **2011**, *50*, 9697. (b) Li, X.; Choy, W. C. H.; Huo, L.; Xie, F.; Sha, W. E. I.; Ding, B.; Guo, X.; Li, Y.; Hou, J.; You, J.; Yang, Y. *Adv. Mater.* **2012**, *24*, 3046.

(12) (a) Kitamura, C.; Tanaka, S.; Yamashita, Y. *Chem. Mater.* **1996**, *8*, 570. (b) Wong, W. Y.; Wang, X. Z.; He, Z.; Djurišić, A. B.; Yip, C. T.; Cheung, K. Y.; Wang, H.; Mak, C. S. K.; Chan, W. K. *Nat. Mater.* **2007**, *6*, 521.

(13) Scharber, M. C.; Mühlbacher, D.; Koppe, M.; Denk, P.; Waldauf, C.; Heeger, A. J.; Brabec, C. J. *Adv. Mater.* **2006**, *18*, 789.

(14) (a) Balaban, T. S. *Acc. Chem. Res.* **2005**, *38*, 612. (b) Imahori, H. *J. Phys. Chem. B* **2004**, *108*, 6130. (c) Liu, Y.; Guo, X.; Xiang, N.; Zhao, B.; Huang, H.; Li, H.; Shen, P.; Tan, S. *J. Mater. Chem.* **2010**, *20*, 1140. (c) Wong, W. K.; Zhu, X.; Wong, W. Y. *Coord. Chem. Rev.* **2007**, *251*, 2386. (d) Wong, W. Y.; Harvey, P. D. *Macromol. Rapid Commun.* **2010**, *31*, 671.

(15) Matsuo, Y.; Sato, Y.; Niinomi, T.; Soga, I.; Tanaka, H.; Nakamura, E. *J. Am. Chem. Soc.* **2009**, *131*, 16048.

(16) Yella, A.; Lee, H. W.; Tsao, H. N.; Yi, C.; Chandiran, A. K.; Nazeeruddin, M. K.; Diau, E. W. G.; Yeh, C. Y.; Zakeeruddin, S. M.; Grätzel, M. *Science* **2011**, *334*, 629.

(17) Umeyama, T.; Takamatsu, T.; Tezuka, N.; Matano, Y.; Araki, Y.; Wada, T.; Yoshikawa, O.; Sagawa, T.; Yoshikawa, S.; Imahori, H. *J. Phys. Chem. C* **2009**, *113*, 10798.

(18) Xiang, N.; Liu, Y.; Zhou, W.; Huang, H.; Guo, X.; Tan, Z.; Zhao, B.; Shen, P.; Tan, S. *Eur. Polym. J.* **2010**, *46*, 1084.

(19) Lee, J.; Song, H.; Lee, S.; Lee, J.; Moon, D. *Eur. Polym. J.* **2011**, *47*, 1686.

(20) Zhou, W.; Shen, P.; Zhao, B.; Jiang, P.; Deng, L.; Tan, S. *J. Polym. Sci., Part A: Polym. Chem.* **1994**, *32*, 1113.

(21) Huang, X.; Zhu, C.; Zhang, S.; Li, W.; Guo, Y.; Zhan, X.; Liu, Y.; Bo, Z. *Macromolecules* **2008**, *41*, 6895.

(22) Lamare, S.; Aly, S. M.; Fortin, D.; Harvey, P. D. *Chem. Commun.* **2011**, *47*, 10942.

(23) Zhan, H.; Lamare, S.; Ng, A.; Kenny, T.; Guernon, H.; Chan, W.; Djurisic, A. B.; Harvey, P. D.; Wong, W. *Macromolecules* **2011**, *44*, 5155.

(24) Gouterman, M. *J. Mol. Spectrosc.* **1961**, *6*, 138.

(25) Anderson, H. L. *Chem. Commun.* **1999**, 2323.

(26) (a) Crossley, M. J.; Burn, P. L. *J. Chem. Soc., Chem. Commun.* **1987**, 39. (b) Crossley, M. J.; Burn, P. L.; Chew, S. S.; Cuttance, F. B.; Newsom, I. A. *J. Chem. Soc., Chem. Commun.* **1991**, 1564. (c) Crossley, M. J.; Burn, P. L.; Langford, S. J.; Pyke, S. M.; Stark, A. G. *J. Chem. Soc., Chem. Commun.* **1991**, 1567. (d) Crossley, M. J.; Burn, P. L. *J. Chem. Soc., Chem. Commun.* **1991**, 1569. (e) Crossley, M. J.; Burn, P. L.; Langford, S. J.; Prashar, J. K. *J. Chem. Soc., Chem. Commun.* **1995**, 1921. (f) Crossley, M. J.; Govenlock, L. J.; Prashar, J. K. *J. Chem. Soc., Chem. Commun.* **1995**, 2379.

(27) (a) Fukuzumi, S.; Ohkubo, K.; E, W.; Ou, Z.; Shao, J.; Kadish, K. M.; Hutchison, J. A.; Ghiggino, K. P.; Sintic, P. J.; Crossley, M. J. *J. Am. Chem. Soc.* **2003**, *125*, 14984. (b) Ou, Z.; E, W.; Shao, J.; Burn, P. L.; Sheehan, C. S.; Walton, R.; Kadish, K. M.; Crossley, M. J. *J. Porphyrins Phthalocyanines* **2005**, *9*, 142. (c) Fukuzumi, S.; Ohkubo, K.; Zhu, W.; Sintic, M.; Khoury, T.; Sintic, P. J.; E, W.; Ou, Z.; Crossley, M. J.; Kadish, K. M. *J. Am. Chem. Soc.* **2008**, *130*, 9451. (d) E, W.; Kadish, K. M.; Sintic, P. J.; Khoury, T.; Govenlock, L. J.; Ou, Z.; Shao, J.; Ohkubo, K.; Reimers, J. R.; Fukuzumi, S.; Crossley, M. J. *J. Phys. Chem. A* **2008**, *112*, 556. (e) Kadish, K. M.; E, W.; Sintic, P. J.; Ou, Z.; Shao, J.; Ohkubo, K.; Fukuzumi, S.; Govenlock, L. J.; McDonald, J. A.; Try, A. C.; Cai, Z. L.; Reimers, J. R.; Crossley, M. J. *J. Phys. Chem. B* **2007**, *111*, 8762. (f) Sintic, P. J.; E, W.; Ou, Z.; Shao, J.; McDonald, J. A.; Cai, Z. L.; Kadish, K. M.; Crossley, M. J.; Reimers, J. R. *Phys. Chem. Chem. Phys.* **2008**, *10*, 515. (g) Hutchison, J. A.; Sintic, P. J.; Crossley, M. J.; Nagamura, T.; Ghiggino, K. P. *Phys. Chem. Chem. Phys.* **2009**, *11*, 3478.

(28) Shi, S.; Wang, X.; Sun, Y.; Chen, S.; Li, X.; Li, Y.; Wang, H. *J. Mater. Chem.* **2012**, *22*, 11006.

(29) (a) Wong, W. Y.; Wang, X. Z.; He, Z.; Chan, K. K.; Djurišić, A. B.; Cheung, K. Y.; Yip, C. T.; Ng, A. M. C.; Xi, Y. Y.; Mak, C. S. K.; Chan, W. K. *J. Am. Chem. Soc.* **2007**, *129*, 14372. (b) Liu, L.; Ho, C. L.; Wong, W. Y.; Cheung, K. Y.; Fung, M. K.; Lam, W. T.; Djurišić, A. B.; Chan, W. K. *Adv. Funct. Mater.* **2008**, *18*, 2824. (c) Wong, W. Y.; Chow, W. C.; Cheung, K. Y.; Fung, M. K.; Djurišić, A. B.; Chan, W. K. *J. Organomet. Chem.* **2009**, *694*, 2717. (d) Wong, W. Y.; Wang, Q. *Polym. Chem.* **2011**, *2*, 432. (e) Chawdhury, N.; Köhler, A.; Friend, R. H.; Wong, W. Y.; Lewis, J.; Younus, M.; Raithby, P. R.; Corcoran, T. C.; Al-Mandhary, M. R. A.; Khan, M. S. *J. Chem. Phys.* **1999**, *110*, 4963. (f) Li, K. C.; Huang, J. H.; Hsu, Y. C.; Huang, P. J.; Chu, C. W.; Lin, J. T.; Ho, K. C.; Wei, K. H.; Lin, H. C. *Macromolecules* **2009**, *42*, 3681. (g) Wang, J. Y.; Hau, S. K.; Yip, H. L.; Davies, J. A.; Chen, K. S.; Zhang, Y.; Sun, Y.; Jen, A. K. Y. *Chem. Mater.* **2011**, *23*, 765. (h) Sun, Y.; Chien, S. C.; Yip, H. L.; Zhang, Y.; Chen, K. S.; Zeigler, D. F.; Chen, F. C.; Lin, B. P.; Jen, A. K. Y. *J. Mater. Chem.* **2011**, *21*, 13247. (i) Ding, P.; Zhong, C.; Zou, Y.; Pan, C.; Wu, H.; Cao, Y. *J. Phys. Chem. C* **2011**, *115*, 16211.

(30) Wong, W. W. H.; Khoury, T.; Vak, D.; Yan, C.; Jones, D. J.; Crossley, M. J.; Holmes, A. B. *J. Mater. Chem.* **2010**, *20*, 7005.

(31) (a) Li, Y. F.; Cao, Y.; Gao, J.; Wang, D. L.; Yu, G.; Heeger, A. J. *Synth. Met.* **1999**, *99*, 243. (b) Wang, X.; Sun, Y.; Chen, S.; Guo, X.; Zhang, M.; Li, X.; Li, Y.; Wang, H. *Macromolecules* **2012**, *45*, 1208.

(32) Lee, W.; Son, S.; Kim, K.; Lee, S.; Shin, W.; Moon, S.; Kang, I. *Macromolecules* **2012**, *45*, 1303.

(33) Schmidt, M. W.; Baldridge, K. K.; Boatz, J. A.; Elbert, S. T.; Gordon, M. S.; Jensen, J. H.; Koseki, S.; Matsunaga, N.; Nguyen, K. A.; Su, S. J.; Windus, T. L.; Dupuis, M.; Montgomery, J. A. *J. Comput. Chem.* **1993**, *14*, 1347.

(34) Pappenfus, T. M.; Schneiderman, D. K.; Casado, J.; López Navarrete, J. T.; Ruiz Delgado, M. C.; Zotti, G.; Vercelli, B.; Lovander, M. D.; Hinkle, L. M.; Bohnsack, J. N.; Mann, K. R. *Chem. Mater.* **2011**, *23*, 823.

(35) (a) Chen, Y.; Huang, W.; Li, C.; Bo, Z. *Macromolecules* **2010**, *43*, 10216. (b) Chen, C. H.; Hsieh, C. H.; Dubose, M.; Cheng, Y. J.; Hsu, C. S. *Macromolecules* **2010**, *43*, 697. (c) Cho, C.; Kang, H.; Kang, T. E.; Cho, H.; Yoon, S.; Jeon, M.; Kim, B. J. *Chem. Commun.* **2011**, *47*, 3577.